Research Square

Preprints are preliminary reports that have not undergone peer review.
They should not be considered conclusive, used to inform clinical practice,
or referenced by the media as validated information.

Tracking host-microbe interactions and bacterial dynamics above a cell monolayer in a label-free real-time manner

Genevieve Schleyer

G.Schleyer@liverpool.ac.uk

University of Liverpool

Eann A. Patterson

University of Liverpool

Judith M. Curran

University of Liverpool

Article

Keywords: host-microbe interaction, nanoscale, transport, label free, microscopy

Posted Date: November 19th, 2026

DOI: https://doi.org/10.21203/rs.3.rs-11430863/v1

License: This work is licensed under a Creative Commons Attribution 4.0 International License.
Read Full License

Additional Declarations: No competing interests reported.

Tracking host-microbe interactions and bacterial dynamics above a cell monolayer in a label-free real-time manner

Genevieve Schleyer*[1], Eann A. Patterson[2] and Judith M. Curran[1]

[1]Department of Materials, Design & Manufacturing Engineering, University of Liverpool, Brownlow Hill, Liverpool, UK

[2]Department of Mechanical and Aerospace Engineering, University of Liverpool, Brownlow Hill, Liverpool, UK

Key words: host-microbe interaction, nanoscale, transport, label free, microscopy

*Corresponding author: G.Schleyer@liverpool.ac.uk

Abstract

Visualising bacterial dynamics near host cells is essential for understanding early colonisation, biofilm formation, and disease progression. However, real-time investigation of host-microbe interactions remains challenging because many imaging methods rely on fluorescent labels that can perturb biological processes and restrict long-term observation. Here, we apply caustics-based imaging, a simple label-free optical microscopy technique, to visualise and track individual oral bacteria at and above living human gingival fibroblast (HGF) monolayers. Using *Streptococcus sanguinis* and *Porphyromonas gingivalis* as model organisms, we demonstrate simultaneous imaging of bacteria and host-cell morphology without labels, enabling bacterial localisation and movement to be monitored within the host cell-proximal environment. The technique resolved diverse behaviours, including free diffusion, confined motion, and surface-associated interactions on both abiotic and cellular substrates. Quantitative tracking showed reduced bacterial mobility near the HGF surface and increasingly Brownian motion with distance from the cell layer, indicating that the host-cell environment modulates microbial dynamics. Bacterial behaviour could also be examined above both unstimulated and inflammatory cell monolayers, demonstrating the versatility of the approach. These findings establish caustics imaging as a powerful platform for real-time, label-free investigation of host-microbe interactions, bacterial attachment, and early biofilm-related processes.

Introduction

The oral cavity hosts a diverse and highly dynamic microbial community comprising hundreds of bacterial species that contribute to oral homeostasis [1]. Many members of this microbiota play beneficial roles in maintaining healthy ecology and preventing colonisation by pathogenic microorganisms. However, disruption of this balance through host pre-disposition to gingival inflammation, lifestyle factors, systemic inflammation, trauma or underlying disease can lead to microbial dysbiosis and the development of oral disease [2].

Periodontal diseases are some of the most prevalent chronic inflammatory conditions worldwide, affecting 20–50% of the population and can result in destruction of the supporting tissues of the teeth, tooth loss and reduced quality of life [3]. Inflammation of the gingival tissue due to accumulation of oral biofilms (plaque), also known as gingivitis, is common amongst the population and can be reversed by implementing improved oral hygiene methods including mechanical plaque removal such as brushing and flossing. However, if left untreated

gingivitis can progress to periodontitis, an irreversible and destructive condition [4]. Periodontitis has also been associated with a variety of systemic conditions, including cardiovascular disease, chronic inflammatory disorders and type 2 diabetes [5-7].

Antimicrobial agents are incorporated into toothpastes and mouthwashes to supplement mechanical plaque removal which help to inhibit biofilm growth. These agents are therefore key measures to prevent serious periodontal disease. In oral hygiene products, antimicrobial agents can directly inhibit growth, alter metabolic processes and disrupt adhesion capabilities [8].

Most studies of microbe-surface interactions rely on endpoint measurements using techniques such as colony counting and quartz crystal microbalance (QCM) [9]. Techniques such as atomic force microscopy (AFM) and optical tweezers can provide information on adhesion forces at the single-cell level but not dynamic attachment behaviour [10,11]. Studies investigating bacterial attachment and behaviour at host-cell interfaces have predominantly relied on fluorescence microscopy to distinguish bacteria from underlying cellular structures since cellular interfaces present a complex and dynamic environment [12-14]. Consequently, relatively little is known about bacterial behaviour within the fluid layer immediately above host tissues where initial encounters and early colonisation events occur. In vitro models are needed to assess not only the formation of biofilm on cellular and solid surfaces but the dynamic activity of bacteria in these environments and how antimicrobial agents can affect the behaviour of bacteria. Methodologies that can visualise host-microbe interactions and monitor bacteria as they transition between a free-floating state and attached state are necessary for the continued development of antimicrobial technologies.

In this study, we apply caustics-based imaging to investigate the behaviour of oral bacteria in the presence of human gingival fibroblasts. Caustics microscopy [15] is based on a natural optical phenomena in which light reflected or refracted off curved surfaces produces concentrated regions of bright light and corresponding regions of shadow. Using a standard inverted optical microscope with some simple adjustments, this optical phenomenon allows objects down to the nanoscale to be visualised and tracked in solution without the need for fluorescent labelling. Using *S. sanguinis* and *P. gingivalis* as model organisms, we demonstrate the ability of the technique to visualise and track individual bacteria in a completely label-free manner both at the cellular surface and within the fluid layer immediately above living cells. By quantifying bacterial diffusion and surface-associated behaviour at different heights relative to the cell layer, we establish a framework for examining bacterial dynamics within the host-cell

proximal microenvironment. These experiments highlight the potential of caustics imaging as a tool for investigating early host-microbe interactions, bacterial attachment processes and the dynamics that precede biofilm formation. We present this tool as a potential platform for in vitro studies investigating the effect of antimicrobial agents on bacterial behaviour.

Methods and materials

Preparation of bacteria cultures

Bacterial cultures of *Streptococcus sanguinis* (*S. sanguinis*) ATCC 10556 and *Porphyromonas gingivalis* (*P. gingivalis*) NCTC 11834 were grown under anaerobic conditions at 37 °C using a 2.5L anaerobic jar (Thermo Fisher Scientific, Loughborough, Leicestershire, UK, Cat No: AG0025A). All cultures were handled aerobically when preparing plates and overnight cultures. Frozen stock of *S. sanguinis* and *P. gingivalis* were transferred from -80 °C freezer to a class II safety cabinet on ice. Columbia Blood agar plates (*S. sanguinis*) and trypticase soy blood agar plates (*P. Gingivalis*) were streaked and incubated in an anaerobic jar at 37 °C for 72 hours and 96 hours, respectively. The resulting cultures of *S. sanguinis* and *P. Gingivalis* were used to inoculate Columbia broth and trypticase soy broth enriched with yeast extract (5 g/L), L-cysteine (0.5 g/L), hemin (5µg/mL) and vitamin K1 (1µg/mL) respectively. Overnight cultures were incubated at 37 °C in an anaerobic jar for a further 72 hours and 96 hours with the lids of the vessels loosened to expose the broth to the environment.

Cell cultures

Human keratinocyte cells, HaCaT (AddexBio, San Diego, CA, USA; cat. no. T0020001) were grown in Dulbecco's Modified Eagle Medium, DMEM with 1g/l glucose (cat. no. 11885084), supplemented with 10% fetal bovine serum, FBS (cat. no. A5256701) and 1% penicillin streptomycin (cat. no. 15070063) purchased from Thermo Fisher Scientific (Loughborough, Leicestershire, UK). Cells were seeded at a density of 12,000 cells/cm^2 with a viability of over 70%, determined using a trypan blue assay, on standard glass cover slips inside a 6-well plate at passage 4-6. Cells were incubated at 37°C with 5% CO_2 and monitored for 96 hours at which point a monolayer had formed.

Human gingival fibroblasts, HGF1, ATCC CRL-2014 were grown in DMEM with 4.5g/l glucose (Thermo Fisher Scientific, Loughborough, Leicestershire, UK Cat No: 11965092), supplemented with 10% FBS and 1% penicillin streptomycin. Cells were seeded at a density of 15,000 cells/cm^2 with a viability of over 70% on standard glass cover slips inside a 6-well plate at

passage 5-7. Cells were incubated at 37°C with 5% CO_2 and monitored for 96 hours at which point a monolayer had formed. Cell monolayers are defined in this study as a cell layer at 90-95% confluence.

Inflammatory response stimulation of human gingival fibroblasts

Human gingival fibroblasts were grown to confluence in complete growth media described above. To stimulate and inflammatory response, cells were treated with lipopolysaccharide (LPS) from *Porphyromonas gingivalis* (Merck Life Science, Gillingham, Dorset, UK; cat. no. SMB00610-1MG) at a working concentration of 1µg/mL diluted in complete growth media for 24 hours. Cells were washed gently with PBS to remove LPS and used for tracking or staining. *P. gingivalis* LPS stimulates the expression of inflammatory cytokines and chemokines and has previously been used in the study of inflammatory responses of human gingival fibroblasts [16-18]. To validate the inflammatory response of the HGF1, interluken-8 (IL-8) levels in cell media were quantified using a human CXCL8/IL-8 ELISA Kit (Proteintech, Manchester, UK; cat. no. KE00006).

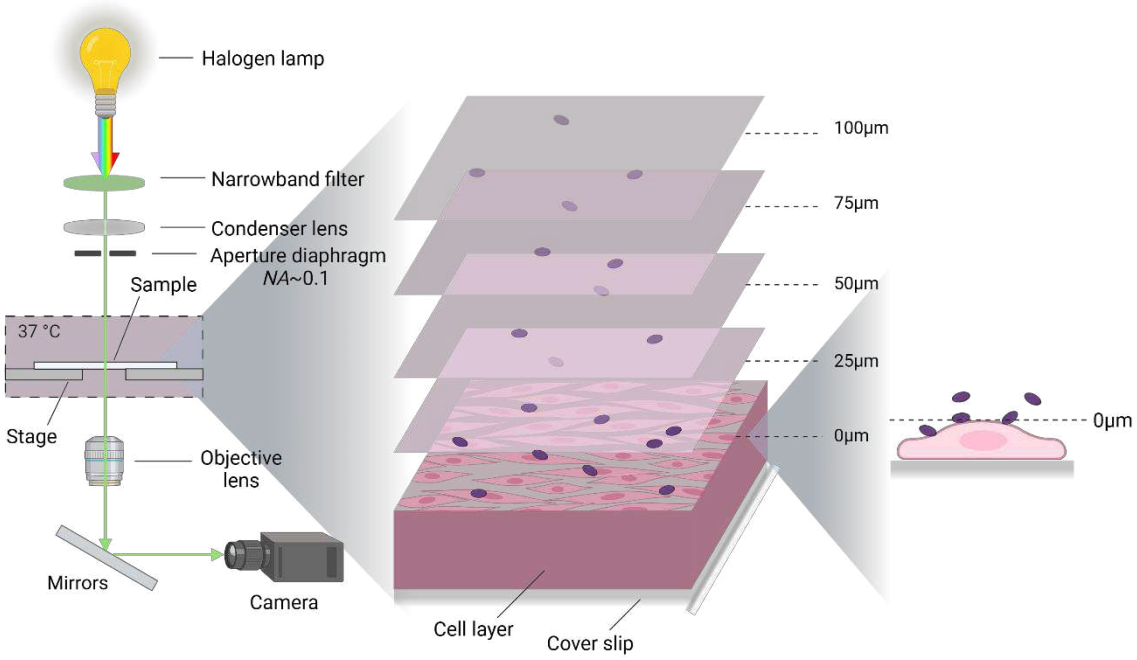
Bacteria tracking

To monitor the interactions of *S. sanguinis* and *P. gingivalis* on standard glass surfaces, overnight cultures were diluted to 10^7 CFU/ml in Columbia broth (*S. sanguinis),* trypticase soy broth enriched with yeast extract (5 g/L), L-cysteine (0.5 g/L), hemin (5µg/mL) and vitamin K1 (1µg/mL) (*P. gingivalis)* or PBS (Both species). 50µl of bacteria solution was placed in a microscope cavity slide (150µm in depth) and covered with a glass cover slip. The sample was upturned in order to monitor the bacteria sedimenting on a flat surface.

To monitor the dynamics of bacteria above cells, overnight cultures of bacteria were diluted to 10^8 CFU/ml in PBS and then further diluted in a 1:10 ratio in filtered DMEM supplemented with 10% FBS to give a final concentration of 10^7 CFU/ml. Microscope slides were prepared in the same way by adding 50µl of the bacteria solution. Cavity wells were sealed with the cell coated glass coverslips and sealed by wiping away excess solution from the edges of the cover slip and sticking with clear nail polish.

Bacterial dynamics and interactions were visualised in a standard inverted optical microscope (Axio Observer Z1, Carl Zeiss, Oberkochen, Germany) in transmission mode with an adjustable aperture in the condenser lens-assembly reduced to a minimum (approx. 1 mm) and narrow band (550 nm) filter. The microscope was set up for Kohler illumination [19]. The schematic in figure 1 demonstrates the experimental set-up. The microscope was equipped with an

incubation stage (Incubator PM S1, Temp and CO_2 module S1, Carl Zeiss, Oberkochen, Germany) which was set at 37 °C throughout. A 40x objective lens together with a camera supported by the ZEN software were used to visualise and record videos of the bacteria. Bacteria dynamics were visualised 15 minutes after contact with the cavity slide. Above the cell layers, bacteria were visualised at four discrete heights as well as directly at the surface of cells.



146 **Figure 1: Bacteria tracking experimental set up.** Experimental set up for tracking bacteria
147 above a cell layer using the caustics methodology. Produced using BioRender.

Bacteria and cell viability

Bacteria were stained with the fluorescent dyes SYTO9 and propidium iodide (PI) from the LIVE/DEAD BacLight kit (Thermo Fisher Scientific, Loughborough, Leicestershire, UK, cat no: L7012) to determine the viability of bacteria and to validate the signatures produced by the caustics microscopy technique. The viability of cells was assessed using trypan blue before seeding and using a LIVE/DEAD viability kit (Fisher Scientific, Loughborough, Leicestershire, UK; cat. no. L3224) after nanoparticle exposure. Cells were seeded with a viability of over 80%. Nanoparticle solutions were exposed to hMSCs on glass coverslips and incubated for two hours at 37°C and 5% CO_2 and the viability of the adherent monolayer evaluated using a live-dead immunofluorescent assay (Fisher Scientific, Loughborough, Leicestershire, UK; cat. no. L3224).

Quantitative analysis

The experimental diffusion coefficient for an object can be obtained from the mean square displacement (MSD) which quantifies the average squared distance travelled by a particle in a certain time [20]. In two dimensions, the MSD at the i^{th} position is expressed as follows [21]:

$$MSD = \frac{1}{N-n}\sum_{i=0}^{N-n}((\Delta x_i(\Delta t))^2 + (\Delta y_i(\Delta t))^2) \quad (1)$$

The mean square displacement, MSD can then be used to calculate an estimate of the diffusion coefficient from the experimental data, using the following expression:

$$D = \frac{MSD}{d(\Delta t)^{\alpha}} \quad (2)$$

where d is the number of dimensions (two in this study), D is the diffusion coefficient and Δt is the time between frames and α is the anomalous diffusion coefficient.

The exponent α was obtained from a linear fit to the log–log plot of MSD versus τ. To minimise bias from statistical noise at long lag times, only the first 25 lag points were used for fitting. Normal diffusion is characterised by a linear relationship between the mean square displacement and time where $\alpha \sim 1$, thus anomalous diffusion is defined as $\alpha \neq 1$. There are various classes of anomalous diffusion but traditionally, it can be divided into at least two subcategories: superdiffusion when $\alpha > 1$ and subdiffusion when $\alpha < 1$. Statistical analysis was performed using a two-tailed Student's t-test, with significance defined as $p < 0.05$.

Results

Validation of Caustics method to visualise S. sanguinis and P. gingivalis

The caustics imaging methodology has previously been validated for monitoring surface interactions of *Escherichia coli* and *Pseudomonas aeruginosa* on coated and uncoated glass surfaces [22]. In the present study, the technique was successfully applied to visualise two oral bacterial species, *Streptococcus sanguinis* and *Porphyromonas gingivalis*, and to characterise their dynamics and interactions at both glass and cellular interfaces. *S. sanguinis* is generally associated with oral health and early biofilm formation, whereas *P. gingivalis* is a recognised periodontal pathogen. They represent organisms occupying distinct ecological and pathogenic roles within the oral microbiome.

The imaging capability of the caustics method to visualise both *S. sanguinis* and *P. gingivalis* was validated by taking consecutive images using the caustics mode and rapidly switching to fluorescence mode (Figures 2-3). No noticeable difference between the caustic images and fluorescent images can be seen meaning the caustics technique is effective at capturing all bacteria in the focus plane. In Figure 2, several *S. sanguinis* chains extended beyond the focal depth of the fluorescence image and appeared out of focus in the corresponding caustics image (white arrows).

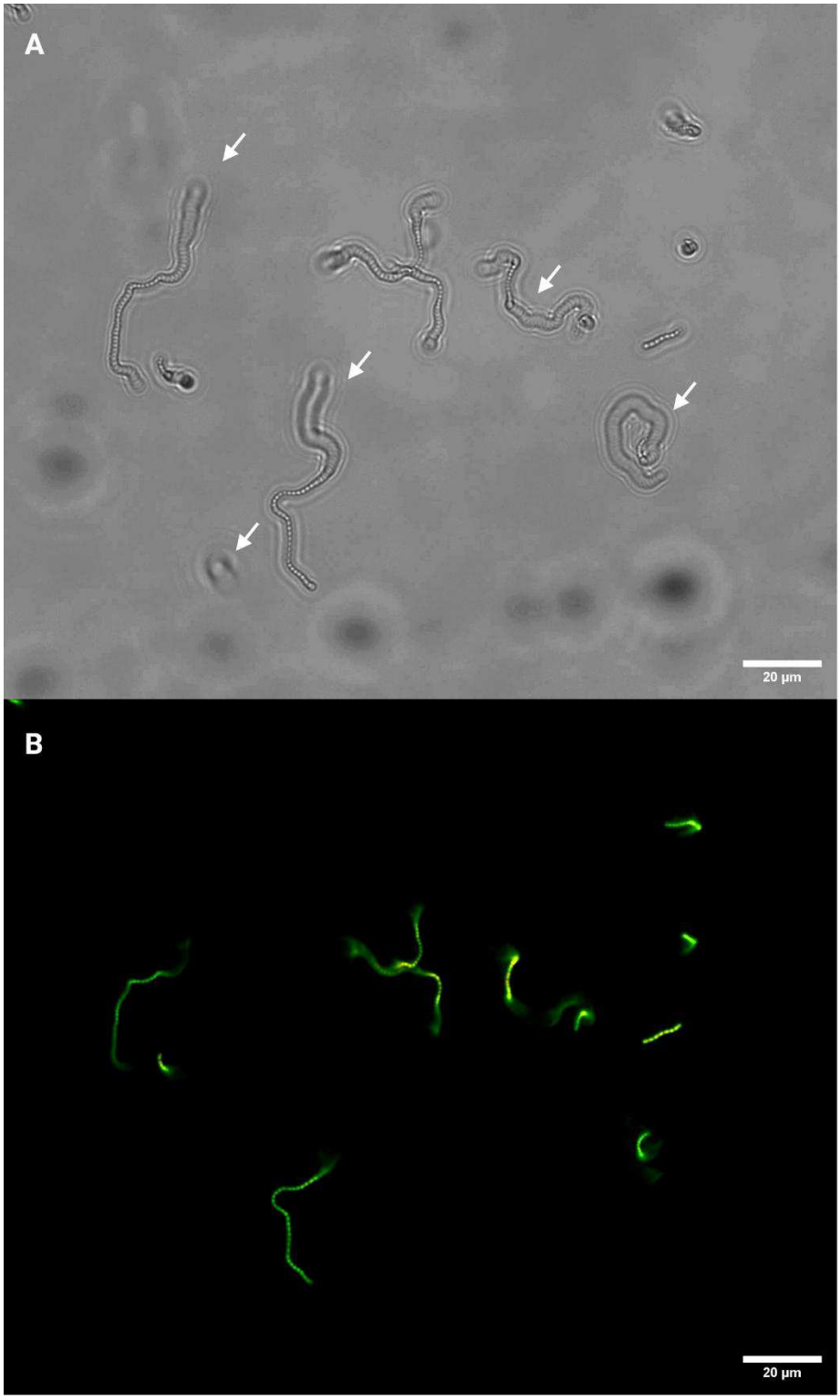


Figure 2: Validation of caustics for visualising *S. sanguinis*. Comparison between the same *S. sanguinis* population adhered to a glass cover slip in saline solution imaged with a.) an inverted optical microscope in caustics mode and b.) fluorescence mode. *Bacteria were stained with the fluorescent dyes SYTO9 and propidium iodide (PI) from the LIVE/DEAD BacLight* kit.

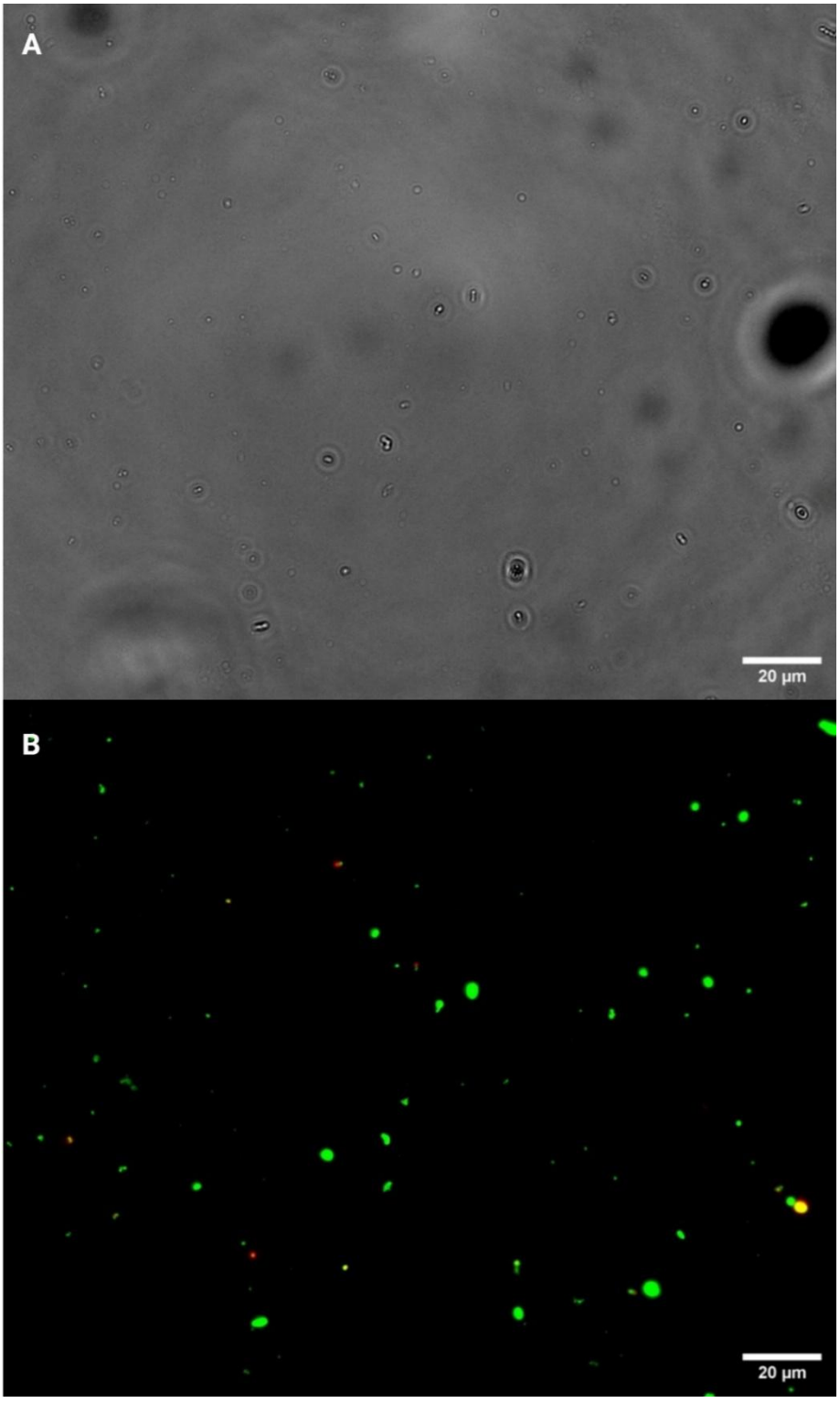


Figure 3: **Validation of caustics for visualising *P. gingivalis*.** *Comparison between the same P. gingivalis population adhered to a glass cover slip in saline solution imaged with a.) an inverted optical microscope in caustics mode and b.) fluorescence mode. Bacteria were stained with the fluorescent dyes SYTO9 and propidium iodide (PI) from the LIVE/DEAD BacLight kit.*

Surface interaction dynamics of S. sanguinis at a glass interface

The dynamics of *S. sanguinis* at standard glass surfaces was tracked in real time. In phosphate-buffered saline (PBS), bacteria were initially observed predominantly as diplococci or short-to-medium length chains exhibiting either unrestricted Brownian-like motion or confined motion near the glass interface (Figure 4). Figure 4b, shows a bacterial chain appearing to be anchored at one end to the glass surface while undergoing a pivoting motion about the attachment point.

Following 2 h incubation in PBS, bacteria were frequently observed in close proximity to the glass coverslip and exhibited little or no measurable motion (Figure 5), consistent with increased surface association. In contrast, bacteria suspended in Columbia broth (CB) and incubated for the same duration displayed lateral sliding motion across the glass surface (Figure 6), suggesting that environmental conditions influenced bacterial surface behaviour.

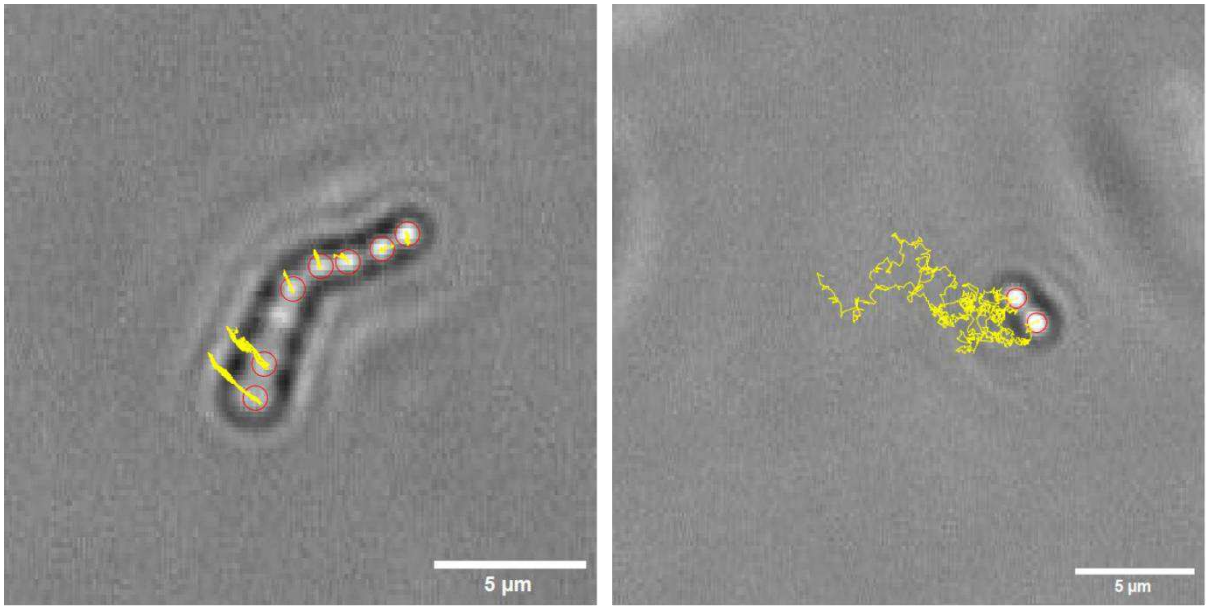


Figure 4: Surface interaction dynamics of *S. sanguinis* in PBS. Tracks (yellow) of S. sanguinis in PBS at a glass surface after 15 minutes inside a microscope slide cavity sealed with a standard glass cover slip a.) displaying freely diffusing motion and b.) showing pivoting motion around a point at which the chain is tethered to the glass surface. The dynamics of the bacteria were monitored for approximately 10s.

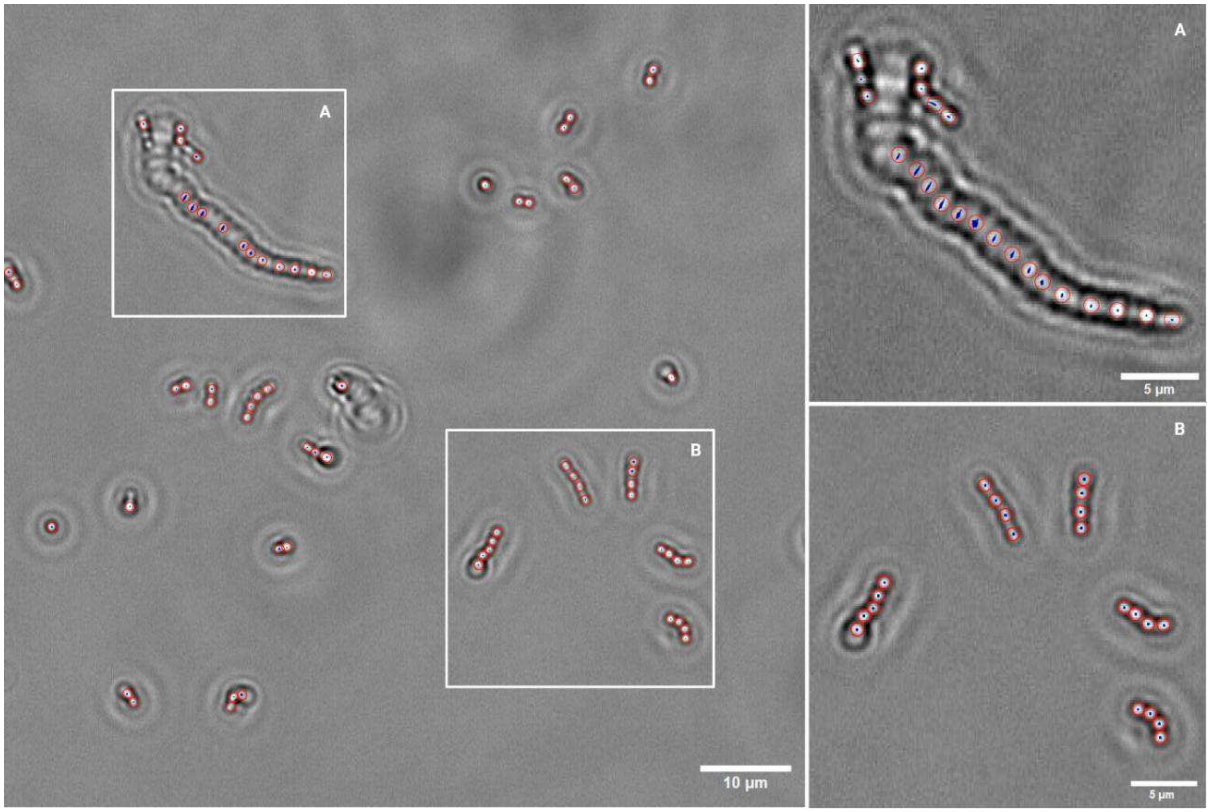


Figure 5: Surface interaction dynamics of *S. sanguinis* in PBS after 2 hours. Tracks (blue) of S. sanguinis in PBS at a glass surface after 2 hours inside a microscope slide cavity sealed with a standard glass cover slip. The dynamics of the bacteria were monitored for approximately 20s.

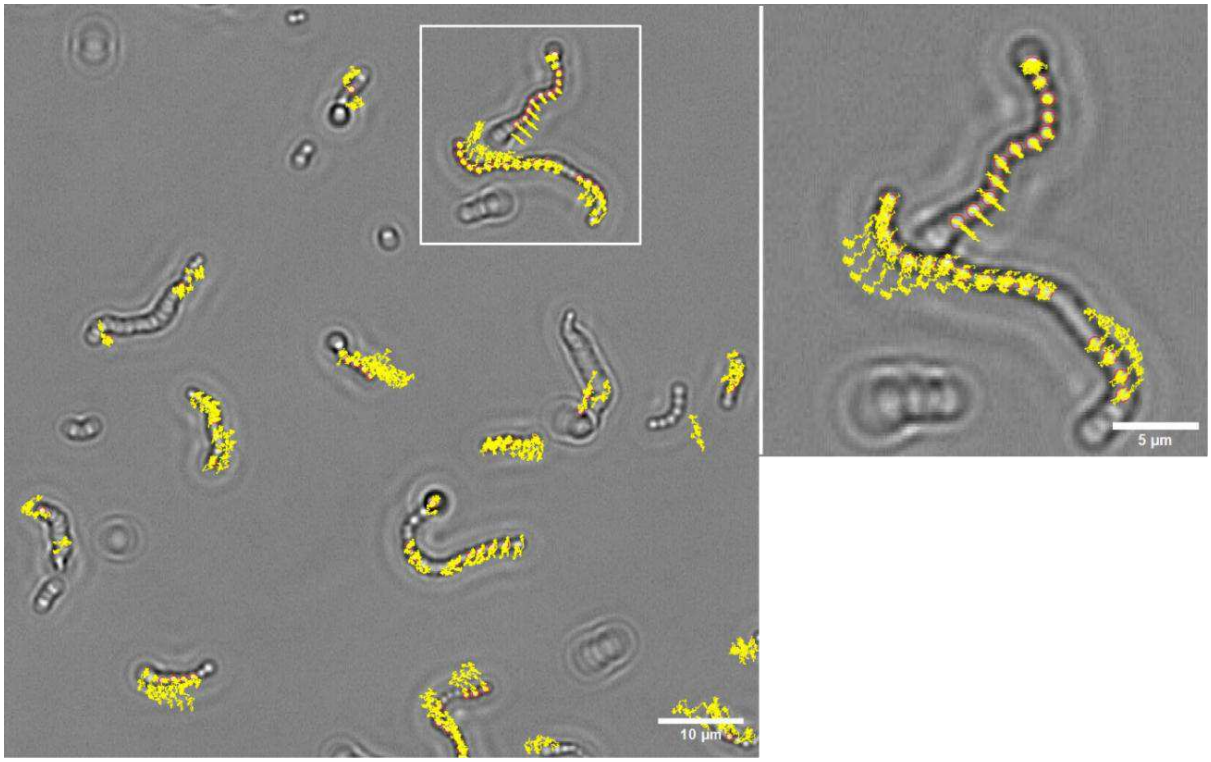


Figure 6: Surface interaction dynamics of *S. sanguinis* in CB after 2 hours. Tracks (yellow) of S. sanguinis in Columbia broth (CB) at a glass surface after 2 hours inside a microscope slide cavity sealed with a standard glass cover slip. The dynamics of the bacteria were monitored for approximately 20s.

Surface interaction dynamics of P. gingivalis at a glass interface

P. gingivalis suspended in tryptic soy broth (TSB) exhibited several distinct behavioural modes over observation periods of 5-10 s. These included confined motion near the glass surface, likely associated with transient adhesion (Figures 7a-b), pivoting motion around apparent attachment points (Figure 7c), and unrestricted Brownian-like trajectories (Figure 7d).

After 2 h incubation, a proportion of bacteria remained statically attached to the glass surface and displayed no discernible motion (Figure 8a). However, other bacteria continued to exhibit Brownian-like diffusion across the substrate (Figure 8b), indicating heterogeneity in surface interactions within the population.

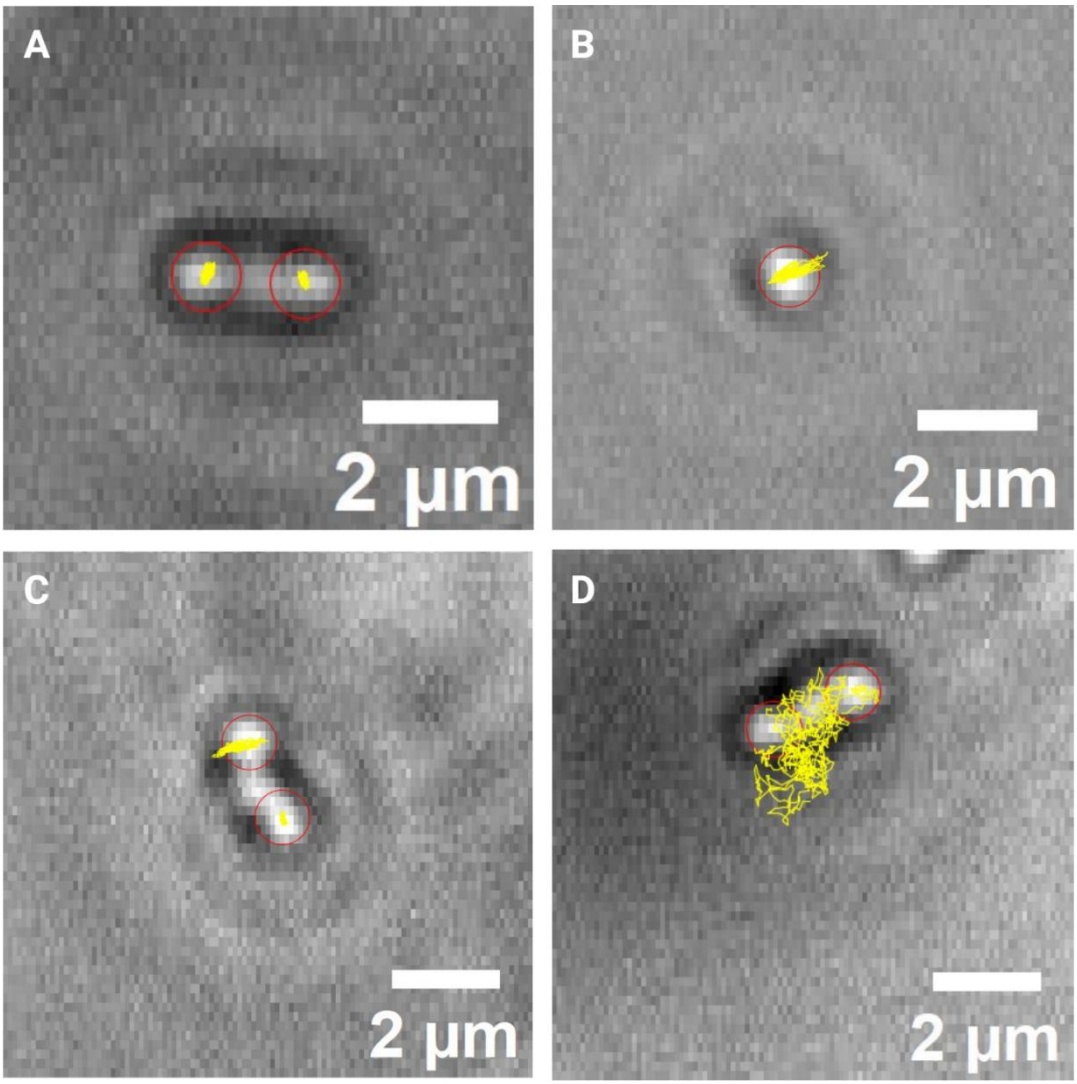


Figure 7: Surface interaction dynamics of *P. gingivalis* in TSB. Tracks (yellow) of P. gingivalis in trypticase soy broth (TSB) enriched with yeast extract (5 g/L), L-cysteine (0.5 g/L), hemin (5µg/mL) and vitamin K1 (1µg/mL) at a glass surface after 15 minutes inside a microscope slide cavity sealed with a standard glass cover slip a.) statically adhered to the surface, b-c.) tethered at one end of the bacterium and d.) showing Brownian motion. The dynamics of the bacteria was monitored for approximately 10s.

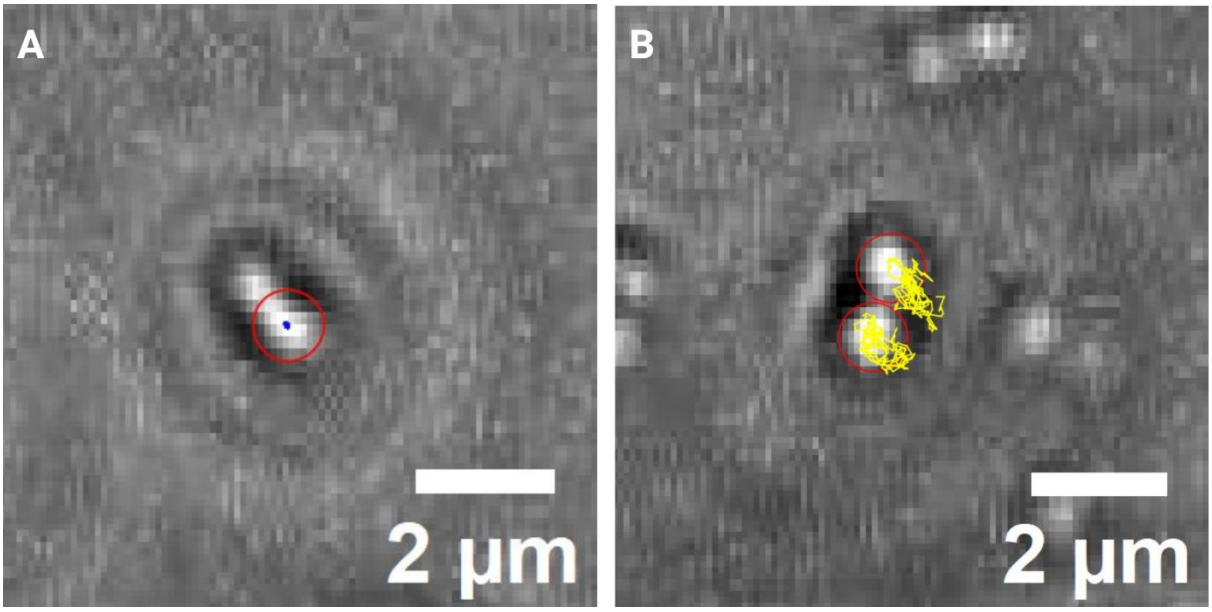


Figure 8: Surface interaction dynamics of *P. gingivalis* in TSB after 2 hours. Tracks (yellow/blue) of P. gingivalis in trypticase soy broth enriched with yeast extract (5 g/L), L-cysteine (0.5 g/L), hemin (5µg/mL) and vitamin K1 (1µg/mL) at a glass surface after 2 hours inside a microscope slide cavity sealed with a standard glass cover slip a.) statically adhered to the surface (blue track) and b.) showing Brownian motion (yellow track). The dynamics of the bacteria were monitored for approximately 10s.

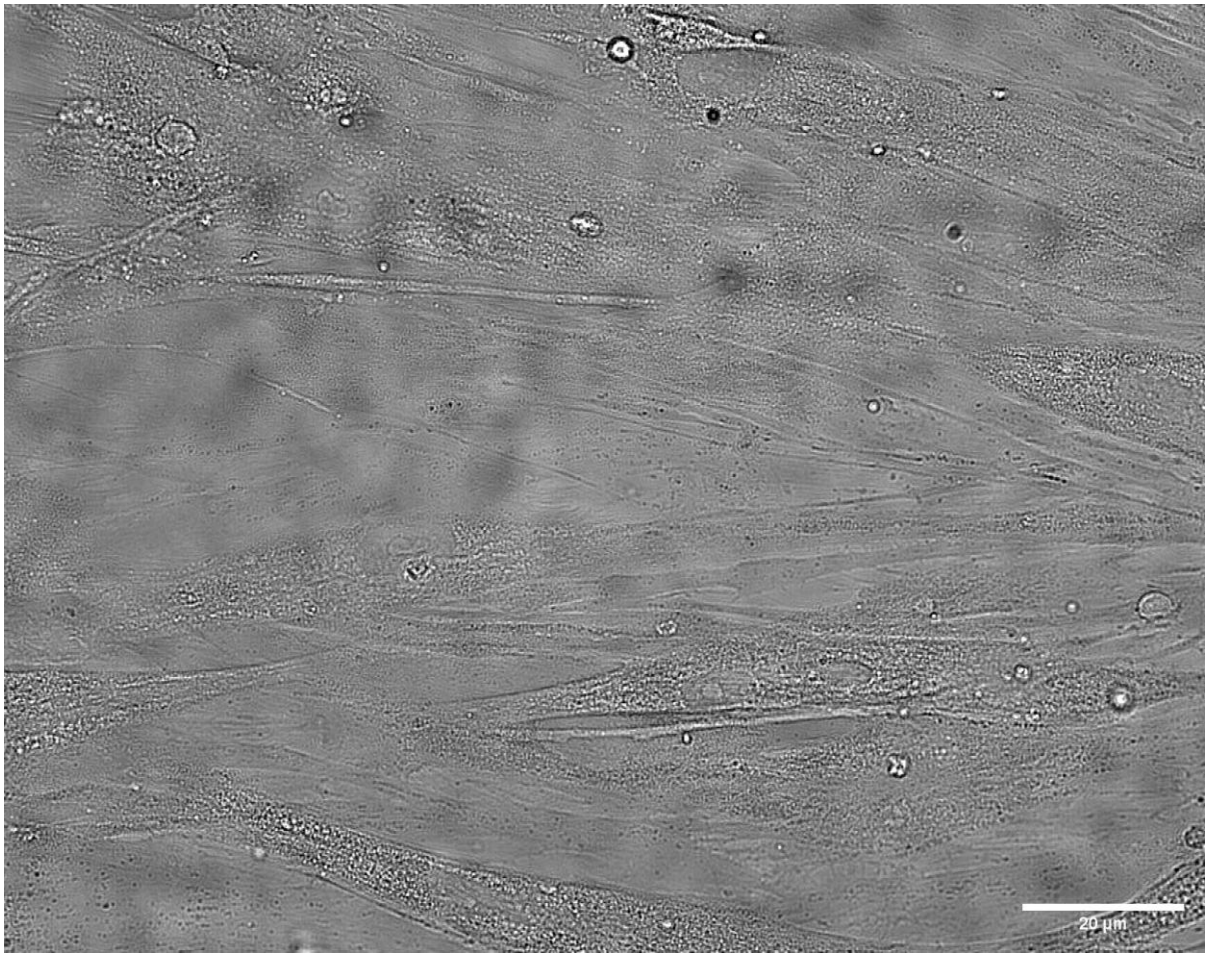
Surface interaction dynamics of P. gingivalis with human gingival fibroblast monolayers

P. gingivalis was visualised in the presence of human gingival fibroblasts (HGFs) maintained in DMEM supplemented with 10% FBS. The ability of the caustics imaging technique to simultaneously visualise both the cellular substrate and bacterial motion immediately adjacent to the cell layer was validated using fluorescence microscopy. Figure 9 shows the caustic signatures produced by the HGFs before addition of bacteria. Figure 10 shows a representative caustics image together with a fluorescence image acquired immediately afterwards. Comparison of the two imaging modes confirmed that bacterial positions and cellular features observed using the caustics approach corresponded closely to those identified by fluorescence imaging.

The morphology of the HGF monolayer was clearly visible within caustics images, enabling the position of individual bacteria to be interpreted relative to cellular structures This provided a means of identifying bacterial attachment events and determining whether bacteria remained associated with the cell surface or continued to diffuse within the surrounding medium. In addition, the ability to visualise both bacteria and cells simultaneously creates the potential to

monitor changes in bacterial localisation in response to alterations in cell morphology or cellular state.

After 15 minutes exposure to the cell layer, *P. gingivalis* exhibited random diffusive motion and confined motion at the cell surface (Figure 11). After 24 hours of co-incubation, a range of behaviours was observed, including diffusive motion, lateral surface-associated movement, and pivoting trajectories (Figure 12). Importantly, bacteria could be visualised both attached to the cell surface and diffusing within the fluid layer above the cells without the need for fluorescent labelling. Live-dead assays showed there was no significant change in cell viability after P. gingivalis had been in contact with the HGF monolayer for 24 hours. Although the overall viability of the cells was not affected by the presence of bacteria, changes in cell function may have occurred which would require more sophisticated assays in future improvements to the model.



277 **Figure 9: Caustics image of human gingival fibroblast monolayer.** Caustics microscopy
278 image of a live human gingival fibroblast monolayer in DMEM supplemented with 10% FBS.

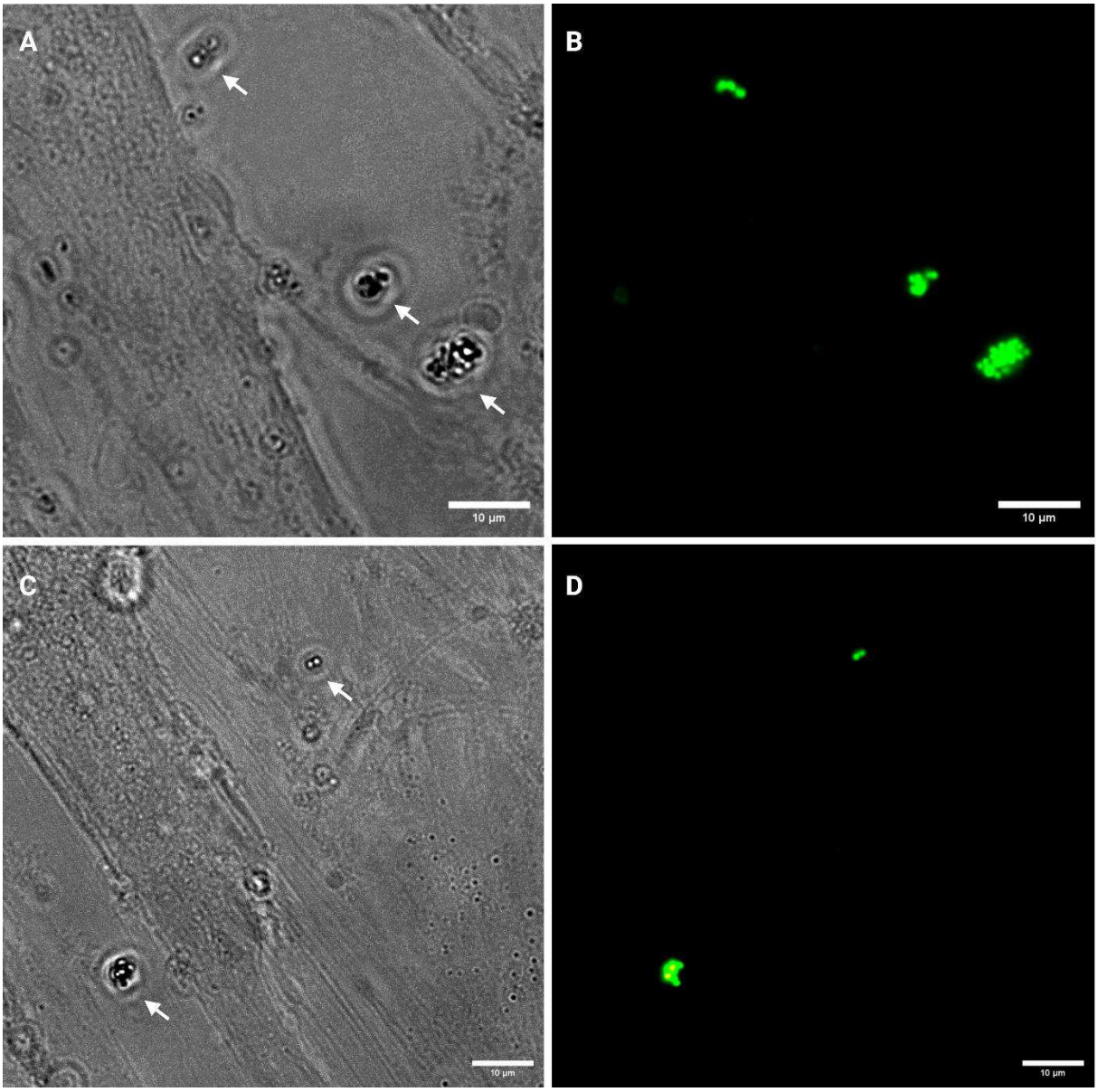


Figure 10: Validation of caustics for visualising *P. gingivalis* at cell interface. P. gingivalis stained with live-dead bacteria viability stain at the surface of human gingival fibroblasts a.) and c.) imaged using caustics mode and b. and d.) corresponding fluorescence signals. White arrows indicate positions of bacteria matching fluorescent signals.

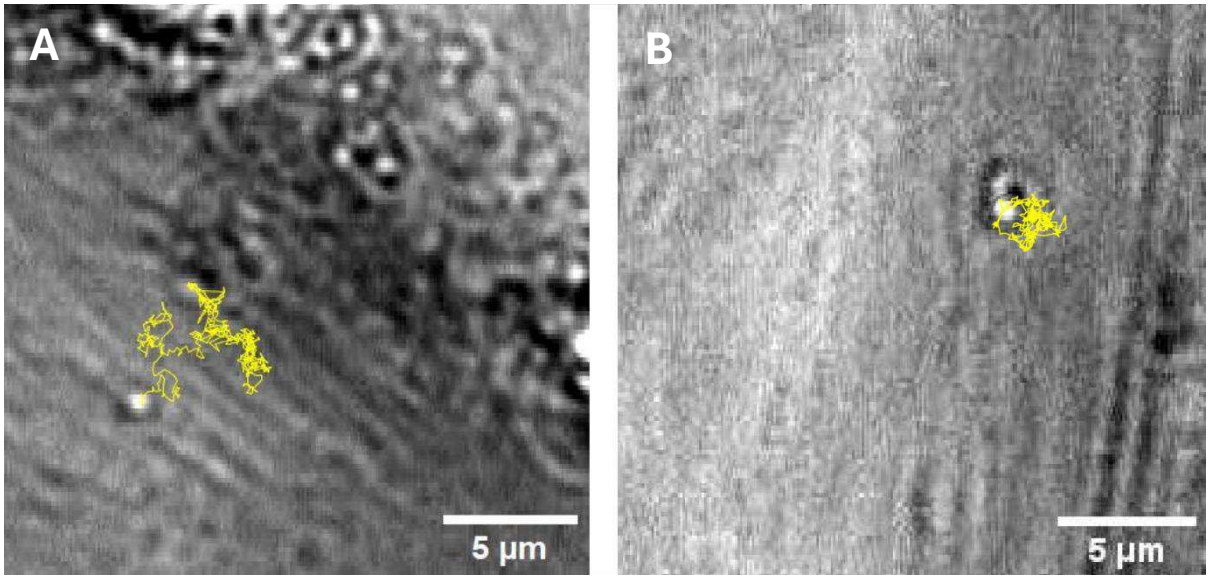


Figure 11: Cell membrane interaction dynamics of *P. gingivalis*. Tracks (yellow) of P. gingivalis at the surface of human gingival fibroblasts 15 min after exposure to the cell layer a.) displaying Brownian motion and b.) confined motion. The dynamics of the bacteria were monitored for approximately 10s.

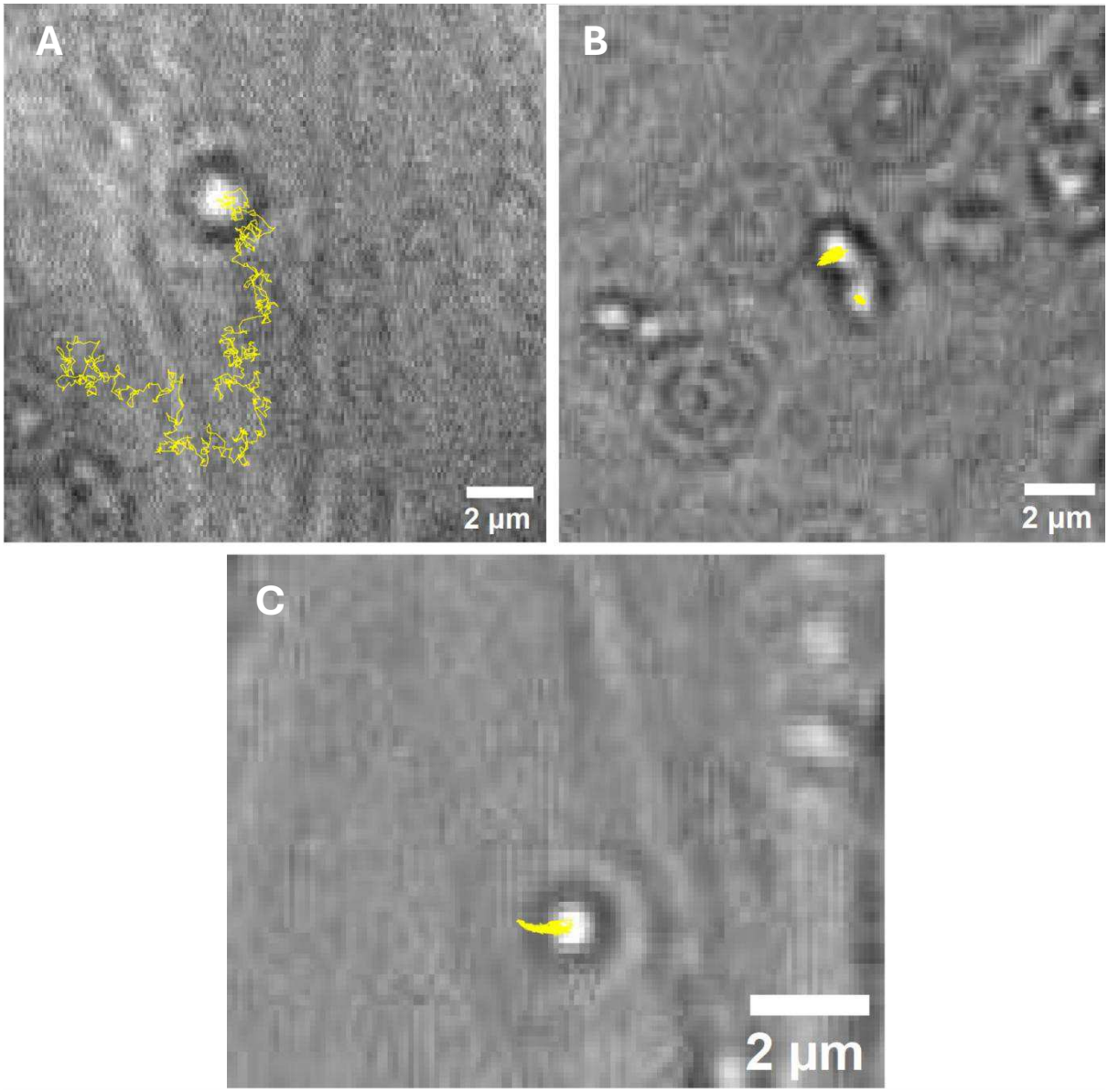


Figure 12: Cell membrane interaction dynamics of *P. gingivalis after 24 hours*. Tracks (yellow) of P. gingivalis at the surface of human gingival fibroblasts 24 hours after exposure to the cell layer a.) displaying Brownian motion and b-c.) confined motion around a point. The dynamics of the bacteria were monitored for approximately 10s.

Apparent diffusion coefficient of P. gingivalis in the presence of human gingival fibroblasts

The trajectories of bacteria were analysed at defined distances above the HGF monolayer to quantify diffusion behaviour as a function of height relative to the cell surface. Track analysis was performed to quantify bacterial displacement and determine diffusion characteristics at different heights relative to the cell layer. Following 15 minutes of incubation, the average diffusion coefficient increased with distance from the cell layer (Figure 13). Bacteria tracked

directly adjacent to the cell surface exhibited significantly lower diffusion coefficients than bacteria tracked 50 µm and 75 µm above the monolayer (50 µm: $p = 0.036$; 75 µm: $p = 0.028$).

After 2 hours of co-incubation, no significant change in diffusivity was observed for bacteria located directly at the cell surface. However, diffusivity increased at greater distances from the monolayer, reaching significance at 50 µm and 75 µm above the cells (50 µm: $p = 0.010$; 75 µm: $p = 0.045$). Consequently, diffusion coefficients measured at 25-100 µm above the cell surface were significantly greater than those recorded directly at the monolayer ($p < 0.001$).

At 24 hours, diffusion coefficients remained elevated relative to the 15 min measurements. Significant increases were observed at 25 µm and 50 µm above the cell layer (50 µm: $p = 0.027$; 75 µm: $p < 0.001$). Diffusion coefficients at all heights between 25 and 100 µm remained significantly greater than those measured directly at the cell surface ($p < 0.001$).

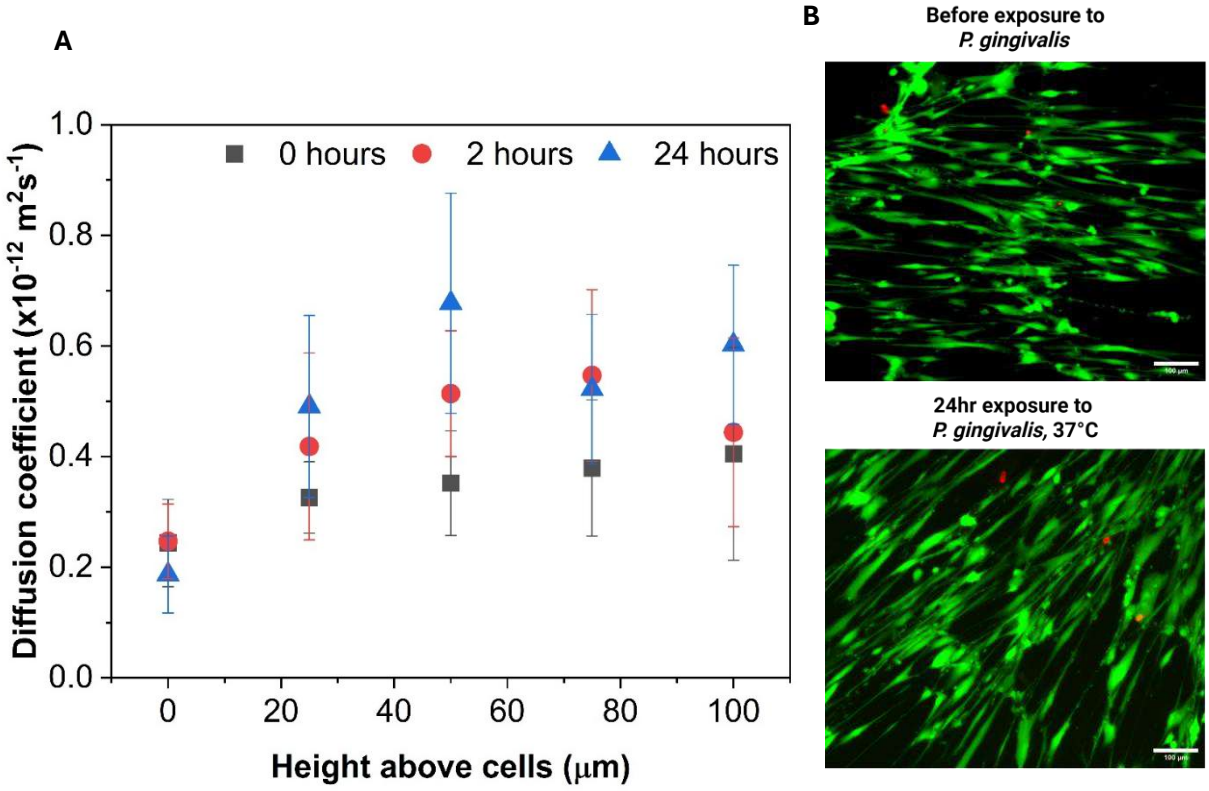


Figure 13: Diffusion coefficient of *P. gingivalis* as a function of height above cells. a.) Average values of experimental diffusion coefficient for P. gingivalis in DMEM with 10% FBS as a function of their height above a human gingival fibroblast monolayer tracked 15 minutes (0 hours), 2 hours and 24 hours after exposure to the monolayer. Error bars represent a half s.d. from the mean (N = 4). b.) Representative images of human gingival fibroblasts stained with live/dead viability stain before and after 24 hours exposure to P. gingivalis.

Alpha exponent of P. gingivalis in the presence of human gingival fibroblasts

After 15 minutes of incubation, the average alpha exponent across all focal planes was 0.94 ± 0.18, indicating slightly subdiffusive behaviour. No significant differences were detected between measurement heights (Figure 14).

Following 2 hours of co-incubation, alpha exponent values remained unchanged (0.96 ± 0.16), indicating that the overall mode of diffusion was stable despite changes in diffusion coefficient.

After 24 hours, bacteria tracked directly at the cell surface exhibited significantly lower alpha exponent values than bacteria measured 25-100 µm above the monolayer (25 µm: $p = 0.025$; 50 µm: $p < 0.001$; 75 µm: $p = 0.0021$; 100 µm: $p = 0.022$). This decrease may reflect an increased proportion of bacteria interacting with or attached to the host cell surface.

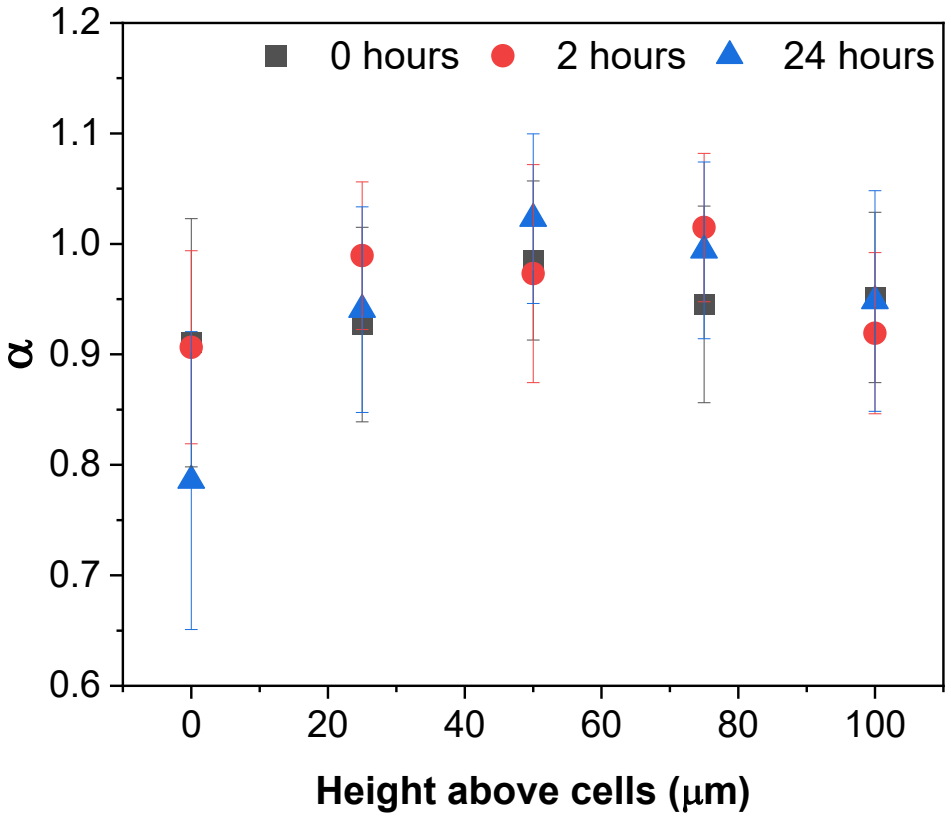


Figure 14: Alpha exponent of *P. gingivalis trajectories* as a function of height above cells. Alpha exponent for P. gingivalis in DMEM with 10% FBS as a function of their height above a human gingival fibroblast monolayer tracked 15 minutes (0 hours), 2 hours and 24 hours after exposure to the monolayer. Error bars represent a half s.d. from the mean (N = 4).

Apparent diffusion coefficient of P. gingivalis in the presence of human gingival fibroblasts stimulated with LPS

The caustics imaging technique was subsequently used to investigate bacterial dynamics in the context of an altered host-cell inflammatory state. HGF monolayers were stimulated with *P. gingivalis*-derived lipopolysaccharide (LPS), which is widely used to induce inflammatory responses in oral cell models. The inflammatory response was confirmed using a human CXCL8/IL-8 ELISA assay. Following stimulation with 1 μg mL^{-1} LPS for 24 h, IL-8 levels showed marked upregulation whereas the control group were below the limit of detection (Figure 15).

Bacterial trajectories were recorded at defined distances above the stimulated HGF monolayer and analysed to determine apparent diffusion coefficients. Similar spatial trends in bacterial diffusivity were observed for both stimulated and unstimulated HGFs, with lower diffusion coefficients detected at the cell surface and greater diffusivity observed at increasing distances

from the monolayer. However, these differences became more pronounced with prolonged incubation above the LPS-stimulated cells (Figure 16).

Following 24 hours of co-incubation, the average diffusion coefficient of bacteria tracked within the fluid phase 25-100 µm above the cell layer was significantly greater than that measured at 15 minutes ($p < 0.001$). In contrast, bacteria tracked directly at the cell surface exhibited a significant reduction in average diffusion coefficient over the same period ($p = 0.016$).

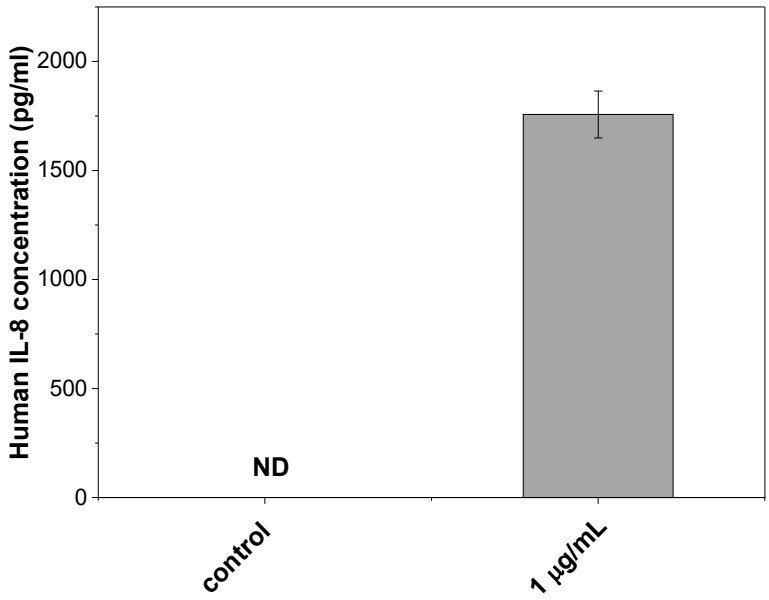


Figure 15: Human IL-8 concentration in cell culture supernatant. Human IL-8 concentration in cell culture supernatant (3 biological replicates, each analysed in duplicate) of human gingival fibroblasts after 24 hours incubation with no LPS and 1µg/ml LPS. ND represents non-detectable values.

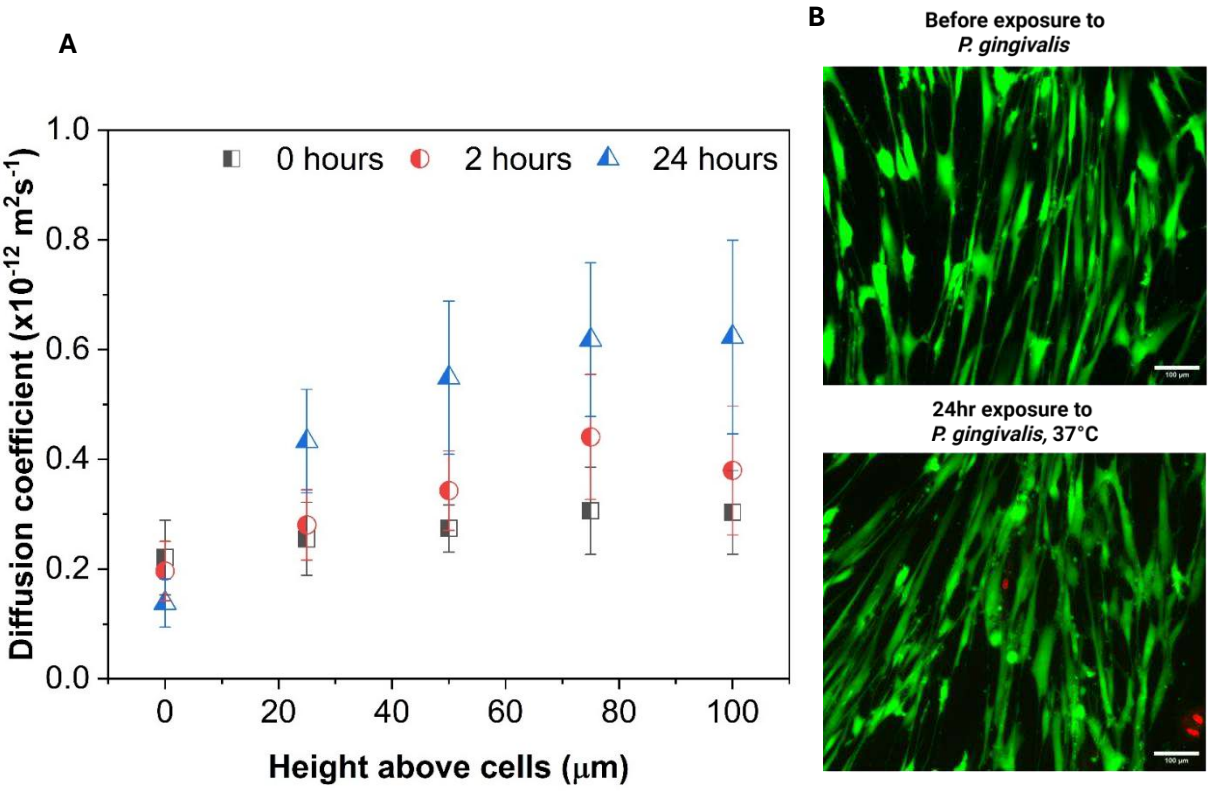


Figure 16: Diffusion coefficient of *P. gingivalis* as a function of height above LPS stimulated cells. a.) Average values of experimental diffusion coefficient for P. gingivalis in DMEM with 10% FBS as a function of their height above a human gingival fibroblast monolayer stimulated for 24 hours with P. gingivalis derived lipopolysaccharide (LPS) tracked 15 minutes (0 hours), 2 hours and 24 hours after exposure to the monolayer. Error bars represent a half s.d. from the mean (N = 4). b.) Representative images of human gingival fibroblasts stimulated for 24 hours with P. gingivalis derived LPS stained with live/dead viability stain before and after 24 hours exposure to P. gingivalis.

Alpha exponent of P. gingivalis in the presence of human gingival fibroblasts stimulated with LPS

No significant differences in alpha exponent values were observed between bacteria tracked above LPS-stimulated HGFs and those tracked above unstimulated cell monolayers. At the 24-hour time point, bacteria located at the cell surface also exhibited significantly lower alpha exponent values than bacteria tracked within the fluid phase above the monolayer (25 μm: $p < 0.001$; 50 μm: $p = 0.0023$; 75 μm: $p < 0.001$; 100 μm: $p = 0.0029$) (Figure 17). This reduction in alpha exponent is consistent with increasingly constrained or subdiffusive motion among bacteria located immediately adjacent to the stimulated cell surface.

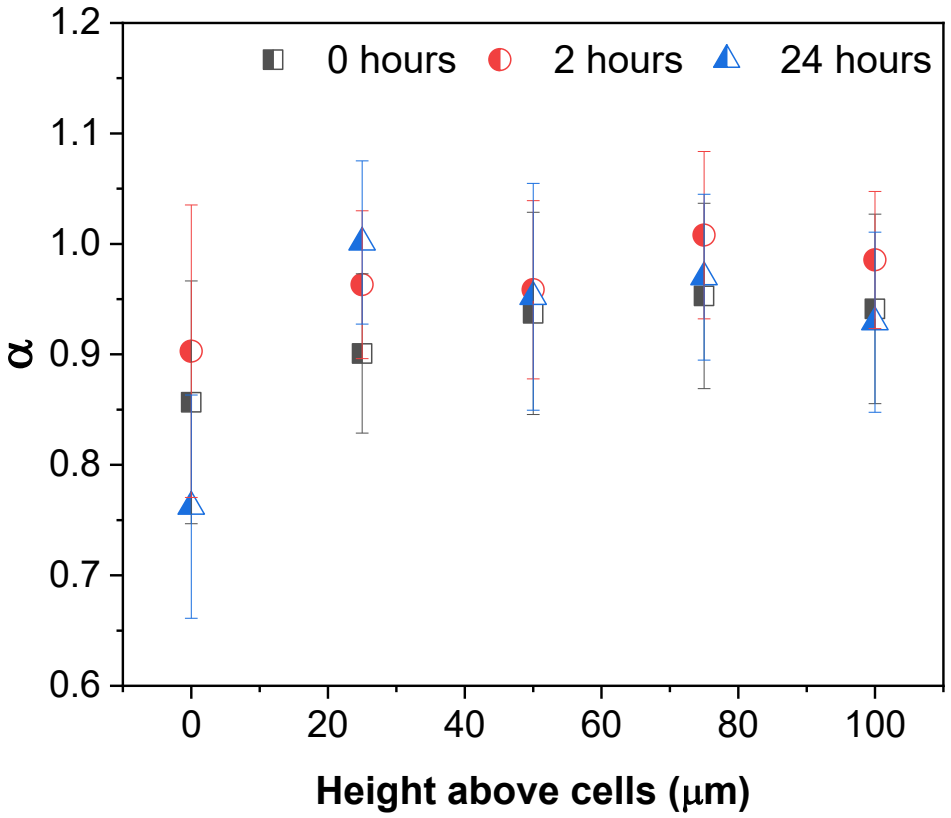


Figure 17: Alpha exponent of *P. gingivalis trajectories* as a function of height above LPS stimulated cells. Alpha exponent for P. gingivalis in DMEM with 10% FBS as a function of their height above a human gingival fibroblast monolayer *stimulated for 24 hours with P. gingivalis derived lipopolysaccharide (LPS)* tracked 15 minutes (0 hours), 2 hours and 24 hours after exposure to the monolayer. Error bars represent a half s.d. from the mean (N = 4).

Discussion

Caustics-based microscopy to track real-time microbe-interface interactions

The ability to visualise and quantify bacterial behaviour in the immediate vicinity of host cells is critical for understanding the early stages of microbial colonisation and biofilm formation. In the present study, we demonstrate that caustics-based imaging enables the label-free visualisation and tracking of individual oral bacteria at both glass and cellular surfaces in real time. Validation against fluorescence microscopy confirmed that the optical signatures generated by both *S. sanguinis* and *P. gingivalis* correspond directly to bacterial cells,

demonstrating that the technique can reliably localise individual bacteria without the need for fluorescent labelling.

Several imaging approaches have previously been used to investigate bacterial dynamics near surfaces, including high-speed bright-field [23], dark-field [24,25], digital holographic [26], phase-contrast [27-29] and differential interference contrast microscopy [30]. These techniques have provided valuable insights into near-surface motility, attachment behaviour, and three-dimensional bacterial trajectories. However, many approaches either require specialised instrumentation, are restricted to a limited distance from the interface or depend on computationally intensive reconstruction methods.

Comparatively fewer studies have tracked individual bacteria at living cell surfaces. Studies investigating bacterial attachment and behaviour at host-cell interfaces have frequently relied on fluorescence microscopy [12-14] to distinguish bacteria from underlying cellular structures since cellular interfaces present a complex and dynamic environment. A limited number of studies have achieved label-free visualisation of microbial behaviour at cellular interfaces. High-definition live-cell DIC microscopy has been used to resolve microbial motility patterns across epithelial monolayers [31] and multimodal holotomography has enabled label-free volumetric imaging of host-pathogen interactions based on refractive-index contrast [32].

In the present study, caustics-based imaging enabled real-time visualisation of individual bacterial interactions at living cellular interfaces without the need for fluorescent labels, eliminating concerns associated with photobleaching, fluorophore toxicity and label-dependent alterations to cellular behaviour, while retaining single-cell resolution.

The caustics-based approach used here also provides a simple, label-free method for detecting and tracking individual bacteria at interfaces and in a fluid phase up to 100μm above the surface in real time. The methodology further enabled tracking of individual bacteria both at the interface and within the surrounding fluid volume up to 100 μm above the surface, thereby allowing transitions between planktonic and surface-associated states to be monitored continuously in a single experiment.

The methodology resolved multiple modes of bacterial behaviour, including unrestricted Brownian-like diffusion, confined diffusion, pivoting trajectories, lateral surface-associated movement and adhesion dynamics. These behaviours were observed on both glass substrates and human gingival fibroblast monolayers, demonstrating the applicability of the approach across both abiotic and biologically relevant surfaces. Cellular interfaces introduce optical

complexity due to variations in surface topography, refractive index and cellular morphology. Despite these challenges, caustics-based imaging maintained sufficient contrast to detect and track individual bacteria at fibroblast monolayers while simultaneously visualising the underlying cellular architecture.

Twitching motility observed is consistent with presence of Type IV pili in S. sanguinis

In phosphate buffered saline (PBS) solution, *S. sanguinis* exhibited both surface-associated and freely diffusing behaviour. After a 2-hour period of contact with the PBS and glass surface, little to no motion was detected suggesting stable attachment to the glass surface. In contrast, bacteria maintained in Columbia broth (CB) remained dynamic over the same time period and frequently displayed intermittent lateral movements characteristic of twitching motility.

Although *S. sanguinis* is generally regarded as non-motile, twitching motility mediated by type IV pili has been reported in several strains and has been implicated in surface exploration, attachment and biofilm development [33,34]. The behaviours observed here are consistent with these previous reports and demonstrate that caustics-based imaging can resolve subtle surface-associated bacterial movements without fluorescent labelling.

The marked reduction in motion observed in PBS compared with nutrient-rich CB also highlights the sensitivity of the technique to environmental influences on bacterial behaviour. While the mechanisms responsible for this transition were not investigated directly, the observations suggest that physiological state and surrounding medium composition influence the extent of surface-associated motion exhibited by S. sanguinis.

Tracking dynamic surface interactions of P. gingivalis

In tryptic soy broth (TSB) growth media, *P. gingivalis* demonstrated a range of behaviours from unrestricted diffusion to apparent surface attachment. Following 2 hours incubation, both mobile and immobilised populations remained present within the field of view, indicating substantial heterogeneity in bacterial behaviour.

As the strain used in this study is classified as non-motile, the observed motion is likely influenced by Brownian forces and interactions with the local microenvironment. Nevertheless, the ability of caustics-based imaging to distinguish freely diffusing, surface-associated and attached bacterial populations highlights its potential for investigating early attachment dynamics in species that do not possess conventional motility mechanisms.

Spatial and temporal heterogeneity in the dynamics of P. gingivalis in the presence of human gingival fibroblasts

P. gingivalis was tracked directly above a human gingival fibroblast (HGF) cell monolayer in Dulbecco's Modified Eagle Medium (DMEM). Quantitative analysis revealed that *P. gingivalis* exhibited reduced apparent diffusivity in the immediate vicinity of the HGF monolayer compared with bacteria tracked within the fluid phase above the cells. This observation is consistent with previous reports that *P. gingivalis* can interact strongly with host-cell surfaces [35,36]. The difference between the cell-associated and fluid-phase populations became more pronounced following prolonged incubation. After 24 h co-incubation, lower diffusion coefficients and reduced α-exponent values were observed at the cell surface, suggesting increasingly constrained and subdiffusive motion near the host-cell interface. This behaviour may reflect enhanced interactions with the cellular surface.

Over time, a significant increase in diffusion rate is seen for bacteria in the fluid phase above the HGF monolayer. Previous studies have shown that it is possible for the dynamic behaviour of certain strains of *P. gingivalis* to evolve over time in response to environmental factors [37,38]. However, these studies were primarily conducted on agar or abiotic surfaces and may not directly translate to the present experimental system. It is therefore possible that changes in the conditioned medium or the local cellular environment contribute to the observed increase in diffusivity. Although live/dead staining indicated minimal cell death after 24 hours, additional measures of cell function and phenotype would be required to determine whether subtle changes in the host-cell environment influenced bacterial dynamics.

Another potential explanation for the elevated diffusion coefficients measured is due to the presence of outer membrane vesicles (OMVs). Gram-negative bacteria, including *P. gingivalis*, produce OMVs 50-250 nm in diameter and are actively released into their surroundings [38,39]. While individual vesicles are considerably smaller than bacterial cells, larger vesicle aggregates could potentially generate caustic signatures comparable to those of the bacteria and contribute to the measured particle population. Future work to distinguish between signatures produced by bacteria and OMVs would contribute to the development of the host-microbe interaction model and open opportunities for investigation into the dynamics of extracellular particles.

Despite changes in diffusion coefficient, the alpha exponent within the fluid phase remained relatively constant over time. This suggests that while bacterial diffusivity may have changed, there was little evidence for a shift in the overall mode of motion i.e. the motion remained

characteristically random. In contrast, the lower alpha exponent values measured at the cell surface are indicative of increasingly constrained dynamics within the immediate vicinity of the HGF monolayer.

Host-cell inflammatory response had no detectable effect on bacterial dynamics

No significant differences were observed in the apparent diffusion coefficients or alpha exponent values of particles tracked above LPS-stimulated HGF monolayers compared with non-stimulated controls. Although a modest reduction in diffusion coefficient was measured for particles located directly at the surface of LPS-stimulated cells, this difference did not reach statistical significance.

The absence of measurable differences between the two conditions may indicate that the inflammatory response induced under the present experimental conditions was insufficient to substantially alter the local environment encountered by *P. gingivalis*. Alternatively, any changes may have been smaller than the sensitivity of the current measurements or masked by biological variability. Consequently, these findings should not be interpreted as evidence that host-cell inflammatory response has no influence on bacterial behaviour.

Nevertheless, these experiments demonstrate that the methodology is sufficiently flexible to investigate bacterial dynamics in the context of changing cellular phenotypes. The ability to perform label-free measurements above living cell populations provides opportunities for future studies examining how a more prolonged inflammatory responses, changes in surface receptor expression, extracellular matrix production, or alterations in cell morphology may influence bacterial interactions with host tissues.

Limitations and future direction

Several limitations of the present study should be acknowledged. First, bacterial interactions were examined using two-dimensional human gingival fibroblast monolayers. While these models provide a reproducible cellular interface, they do not fully capture the complexity of native oral tissues. Future studies should explore the application of caustics-based imaging in more physiologically relevant three-dimensional tissue models, organotypic cultures and organ-on-chip platforms. Similarly, all experiments were conducted under static conditions. As bacterial transport and adhesion in the oral cavity are influenced by fluid flow and mechanical forces, further work is required to evaluate the performance of the technique in dynamic flow environments. Future developments of the caustics microscopy technique could involve

integrating a microfluidics platform into the experimental set up to enable more physiologically relevant studies of host-microbe interactions.

The methodology provides information on bacterial trajectories and dynamic behaviour but does not directly measure adhesion forces or identify the molecular mechanisms governing attachment. Consequently, changes in diffusivity or transitions to confined motion should be interpreted as indicators of altered surface interactions rather than direct measures of specific biological processes. Thus, the caustics tracking technique could be used as a complementary tool for understanding adhesion and surface interaction.

The assessment of host-cell health was limited to live/dead staining. Although minimal cell death was observed throughout the study, additional analyses of cellular function, metabolic activity and inflammatory responses would provide a more comprehensive understanding of how the cellular microenvironment influences bacterial dynamics over extended periods. Furthermore, the maximum time the cells are viable for on the microscope slide has not been established and would require further investigation.

Despite these limitations, the present work demonstrates that caustics-based imaging is a robust and accessible platform for the label-free visualisation of bacterial dynamics at both abiotic and cellular interfaces. The ability to simultaneously track individual bacteria within the fluid phase and at the surface of living cells provides a foundation for future development of the model and studies in increasingly complex and physiologically relevant host-microbe systems.

Conclusions

By enabling label-free visualisation of bacteria within the host cell-proximal microenvironment, caustics imaging provides a new experimental framework for investigating the earliest stages of host-microbe interactions and the processes that ultimately lead to microbial colonisation and biofilm formation. Using *P. gingivalis* and *S. sanguinis* as model organisms, we showed that the technique can resolve bacterial behaviours ranging from free diffusion to confined and surface-associated motion on both abiotic and cellular surfaces. Quantitative analysis revealed reduced bacterial mobility in the immediate proximity of human gingival fibroblasts, highlighting the influence of the host-cell microenvironment on bacterial dynamics. Importantly, caustics imaging simultaneously visualised bacterial cells and host-cell morphology without fluorescent labelling, providing a powerful platform for studying the early stages of host-microbe interactions. These findings establish caustics imaging as a valuable tool for investigating

bacterial attachment, colonisation, and the dynamic processes that precede biofilm formation in physiologically relevant settings.

Author contributions

G.S. performed the experiments, analysed the data and prepared the first draft of the manuscript; J.M.C. and E.A.P. conceived, coordinated and supervised the study, participated in the interpretation of the results and edited the manuscript. All authors gave final approval for publication.

Funding

G.S. was supported by the Biotechnology and Biological Sciences Research Council (BBSRC) and is part of the Collaborative Training Partnership in which the BBSRC is supported by a number of industrial partners.

Data availability

The datasets generated and/or analysed during the current study are available in the Liverpool DataCat repository at: https://doi.org/10.17638/datacat.liverpool.ac.uk%2F3114

Competing interests

The authors declare no competing interests.

References

1 Griffen, A. L. *et al.* Distinct and complex bacterial profiles in human periodontitis and health revealed by 16S pyrosequencing. *The ISME journal* **6**, 1176-1185 (2012).

2 Li, X., Liu, Y., Yang, X., Li, C. & Song, Z. The oral microbiota: community composition, influencing factors, pathogenesis, and interventions. *Frontiers in microbiology* **13**, 895537 (2022).

3 Peng, P., Cai, J., Zhang, L., Lu, Y. & Kuang, P. The subgingival microbiome in periodontitis: from ecological dysbiosis and metabolic reprogramming to precision interventions. *Frontiers in Microbiology* **Volume 17 - 2026**, doi:10.3389/fmicb.2026.1906205 (2026).

4 Hashim, N. T. *et al.* The Global Burden of Periodontal Disease: A Narrative Review on Unveiling Socioeconomic and Health Challenges. *Int J Environ Res Public Health* **22**, doi:10.3390/ijerph22040624 (2025).

5 Kinane, D. F., Stathopoulou, P. G. & Papapanou, P. N. Periodontal diseases. *Nature Reviews Disease Primers* **3**, 17038, doi:10.1038/nrdp.2017.38 (2017).

6 Hashim, N. T. *et al.* The global burden of periodontal disease: a narrative review on unveiling socioeconomic and health challenges. *International journal of environmental research and public health* **22**, 624 (2025).

7 Tattar, R., da Costa, B. D. C. & Neves, V. C. M. The interrelationship between periodontal disease and systemic health. *Br Dent J* **239**, 103-108, doi:10.1038/s41415-025-8642-2 (2025).

8 Rajendiran, M., Trivedi, H. M., Chen, D., Gajendrareddy, P. & Chen, L. Recent Development of Active Ingredients in Mouthwashes and Toothpastes for Periodontal Diseases. *Molecules* **26**, doi:10.3390/molecules26072001 (2021).

9 Gutman, J., Walker, S. L., Freger, V. & Herzberg, M. Bacterial attachment and viscoelasticity: physicochemical and motility effects analyzed using quartz crystal microbalance with dissipation (QCM-D). *Environmental science & technology* **47**, 398-404 (2013).

10 Boks, N. P., Busscher, H. J., van der Mei, H. C. & Norde, W. Bond-strengthening in staphylococcal adhesion to hydrophilic and hydrophobic surfaces using atomic force microscopy. *Langmuir* **24**, 12990-12994 (2008).

11 Beaussart, A. *et al.* Single-cell force spectroscopy of probiotic bacteria. *Biophysical journal* **104**, 1886-1892 (2013).

12 Antypas, H., Zhang, T., Choong, F. X., Melican, K. & Richter-Dahlfors, A. Dynamic single cell analysis in a proximal-tubule-on-chip reveals heterogeneous epithelial colonization strategies of uropathogenic Escherichia coli under shear stress. *FEMS Microbes* **4**, xtad007, doi:10.1093/femsmc/xtad007 (2023).

13 Dewangan, N. K., Mohiuddin, S. G., Sensenbach, S., Karki, P. & Orman, M. A. Uncovering bacterial-mammalian cell interactions via single-cell tracking. *BMC Biology* **22**, 256, doi:10.1186/s12915-024-02056-z (2024).

14 Pierrat, X., Wong, J. P. H., Al-Mayyah, Z. & Persat, A. The Mammalian Membrane Microenvironment Regulates the Sequential Attachment of Bacteria to Host Cells. *mBio* **12**, e0139221, doi:10.1128/mBio.01392-21 (2021).

15 Patterson, E. A. & Whelan, M. P. Optical signatures of small nanoparticles in a conventional microscope. *Small* **4**, 1703-1706 (2008).

16 Jian, C. X. *et al*. Tormentic acid inhibits LPS-induced inflammatory response in human gingival fibroblasts via inhibition of TLR4-mediated NF-κB and MAPK signalling pathway. *Arch Oral Biol* **60**, 1327-1332, doi:10.1016/j.archoralbio.2015.05.005 (2015).

17 Agger, A. E., Hlinkova, J., Reseland, J. E. & Samara, A. 3D models for oral inflammation using gingival fibroblasts, lipopolysaccharides and hypoxia. *Scientific Reports* **16**, 17190, doi:10.1038/s41598-026-47648-7 (2026).

18 Agger, A. E., Samara, A., Geng, T., Olstad, O. K. & Reseland, J. E. Mimicking and in vitro validating chronic inflammation in human gingival fibroblasts. *Arch Oral Biol* **169**, 106113, doi:10.1016/j.archoralbio.2024.106113 (2025).

19 Köhler, A. New method of illumination for photomicrographical purposes. *Journal of the Royal Microscopical Society* **14**, 261-262 (1894).

20 Schirripa Spagnolo, C. & Luin, S. Trajectory Analysis in Single-Particle Tracking: From Mean Squared Displacement to Machine Learning Approaches. *International Journal of Molecular Sciences* **25**, 8660 (2024).

21 Michalet, X. Mean square displacement analysis of single-particle trajectories with localization error: Brownian motion in an isotropic medium. *Physical Review E* **82**, 041914, doi:10.1103/PhysRevE.82.041914 (2010).

22 Giorgi, F., Curran, J. M. & Patterson, E. A. Real-time monitoring of the dynamics and interactions of bacteria and the early-stage formation of biofilms. *Sci Rep* **12**, 18146, doi:10.1038/s41598-022-22669-0 (2022).

23 Yang, X. *et al*. Hydrodynamic and entropic effects on colloidal diffusion in corrugated channels. *Proc Natl Acad Sci U S A* **114**, 9564-9569, doi:10.1073/pnas.1707815114 (2017).

24 Li, G., Tam, L.-K. & Tang, J. X. Amplified effect of brownian motion in bacterial near-surface swimming. *PNAS* **105**, 18355-18359 (2008).

25 Cerbino, R., Piotti, D., Buscaglia, M. & Giavazzi, F. Dark field differential dynamic microscopy enables accurate characterization of the roto-translational dynamics of bacteria and colloidal clusters. *Journal of Physics: Condensed Matter* **30**, 025901 (2018).

26 Molaei, M. & Sheng, J. Imaging bacterial 3D motion using digital in-line holographic microscopy and correlation-based de-noising algorithm. *Opt Express* **22**, 32119-32137, doi:10.1364/oe.22.032119 (2014).

27 Taute, K. M., Gude, S., Tans, S. J. & Shimizu, T. S. High-throughput 3D tracking of bacteria on a standard phase contrast microscope. *Nature Communications* **6**, 8776, doi:10.1038/ncomms9776 (2015).

28 Edwards, M. R., Carlsen, R. W., Zhuang, J. & Sitti, M. Swimming characterization of Serratia marcescens for bio-hybrid micro-robotics. *Journal of Micro-Bio Robotics* **9**, 47-60 (2014).

29 Li, G. & Tang, J. X. Accumulation of microswimmers near a surface mediated by collision and rotational Brownian motion. *Physical review letters* **103**, 078101 (2009).

30 Obara, B., Roberts, M. A., Armitage, J. P. & Grau, V. Bacterial cell identification in differential interference contrast microscopy images. *BMC bioinformatics* **14**, 1-13 (2013).

31 van Rijn Jorik, M. *et al.* High-Definition DIC Imaging Uncovers Transient Stages of Pathogen Infection Cycles on the Surface of Human Adult Stem Cell-Derived Intestinal Epithelium. *mBio* **13**, e00022-00022, doi:10.1128/mbio.00022-22 (2022).

32 Yu, Z. *et al.* Multimodal holotomography for volumetric monitoring of host–pathogen interactions. *BioMedical Engineering OnLine* (2026).

33 Chen, Y. M., Wang, H. Y., Wu, C. H., Lin, Y. J. & Chiu, C. H. Prevalence of Type IV Pili-Mediated Twitching Motility in Streptococcus sanguinis Strains and Its Impact on Biofilm Formation and Host Adherence. *Appl Environ Microbiol* **88**, e0140322, doi:10.1128/aem.01403-22 (2022).

34 Martini, A. M., Moricz, B. S., Woods, L. J. & Jones, B. D. Type IV Pili of Streptococcus sanguinis Contribute to Pathogenesis in Experimental Infective Endocarditis. *Microbiology Spectrum* **9**, e01752-01721, doi:doi:10.1128/Spectrum.01752-21 (2021).

35 Enersen, M., Nakano, K. & Amano, A. Porphyromonas gingivalis fimbriae. *J Oral Microbiol* **5**, doi:10.3402/jom.v5i0.20265 (2013).

36 Bugueno, I. M. *et al.* Porphyromonas gingivalis bypasses epithelial barrier and modulates fibroblastic inflammatory response in an in vitro 3D spheroid model. *Scientific Reports* **8**, 14914, doi:10.1038/s41598-018-33267-4 (2018).

37 Moradali, M. F., Ghods, S., Angelini, T. E. & Davey, M. E. Amino acids as wetting agents: surface translocation by Porphyromonas gingivalis. *The ISME Journal* **13**, 1560-1574, doi:10.1038/s41396-019-0360-9 (2019).

38 Vermilyea, D. M., Moradali, M. F., Kim, H. M. & Davey, M. E. PPAD Activity Promotes Outer Membrane Vesicle Biogenesis and Surface Translocation by Porphyromonas gingivalis. *J Bacteriol* **203**, doi:10.1128/jb.00343-20 (2021).

669 39 Xie, H. Biogenesis and Function of Porphyromonas Gingivalis Outer Membrane
670 Vesicles. *Future Microbiology* **10**, 1517-1527, doi:10.2217/fmb.15.63 (2015).

671